Neurobiology of Disease 150 (2021) 105244

Contents lists available at ScienceDirect

Neurobiology of Disease

journal homepage: www.elsevier.com/locate/ynbdi

Genetic inactivation of the sigma-1 chaperone protein results in decreased expression of the R2 subunit of the GABA-B receptor and increased susceptibility to seizures

Edijs Vavers [a,*], Baiba Zvejniece [a,b], Gundega Stelfa [a,c], Baiba Svalbe [a], Karlis Vilks [a,b], Einars Kupats [a,d], Rudolfs Mezapuke [a], Lasma Lauberte [a], Maija Dambrova [a,d], Liga Zvejniece [a]

[a] Latvian Institute of Organic Synthesis, Riga LV-1006, Latvia
[b] University of Latvia, Riga LV-1586, Latvia
[c] Latvia University of Life Sciences and Technologies, Jelgava LV-3001, Latvia
[d] Riga Stradins University, Riga LV-1007, Latvia

ARTICLE INFO

Keywords:
Sigma-1 receptor
Knockout
GABA-B receptor
Seizures
Medial habenula
NE-100

ABSTRACT

There is a growing body of evidence demonstrating the significant involvement of the sigma-1 chaperone protein in the modulation of seizures. Several sigma-1 receptor (Sig1R) ligands have been demonstrated to regulate the seizure threshold in acute and chronic seizure models. However, the mechanism by which Sig1R modulates the excitatory and inhibitory pathways in the brain has not been elucidated. The aim of this study was to compare the susceptibility to seizures of wild type (WT) and Sig1R knockout (Sig1R−/−) mice in intravenous pentylenetetrazol (PTZ) and (+)-bicuculline (BIC) infusion-induced acute seizure and Sig1R antagonist NE-100-induced seizure models. To determine possible molecular mechanisms, we used quantitative PCR, Western blotting and immunohistochemistry to assess the possible involvement of several seizure-related genes and proteins. Peripheral tissue contractile response of WT and Sig1R−/− mice was studied in an isolated *vasa deferentia* model. The most important finding was the significantly decreased expression of the R2 subunit of the GABA-B receptor in the hippocampus and habenula of Sig1R−/− mice. Our results demonstrated that Sig1R−/− mice have decreased thresholds for PTZ- and BIC-induced tonic seizures. In the NE-100-induced seizure model, Sig1R−/− animals demonstrated lower seizure scores, shorter durations and increased latency times of seizures compared to WT mice. Sig1R-independent activities of NE-100 included downregulation of the gene expression of iNOS and GABA-A γ2 and inhibition of KCl-induced depolarization in both WT and Sig1R−/− animals. In conclusion, the results of this study indicate that the lack of Sig1R resulted in decreased expression of the R2 subunit of the GABA-B receptor and increased susceptibility to seizures. Our results confirm that Sig1R is a significant molecular target for seizure modulation and warrants further investigation for the development of novel anti-seizure drugs.

1. Introduction

Epilepsy is a chronic neurological disease that is characterized by seizures. The seizures could be caused by disturbances at the receptor function and neurotransmission levels, metabolic problems in the central nervous system or some conditions leading to pathological changes in the brain, such as traumatic brain injuries, stroke, status epilepticus or infectious diseases (Alyu and Dikmen, 2017). For the treatment of seizures, heterogeneous groups of antiepileptic drugs (AEDs) are used. However, a number of patients do not fully respond to currently available treatment, and existing AEDs achieve seizure freedom only in approximately two-thirds of patients (Perucca et al., 2018). Therefore, searching for new possible mechanisms and novel AEDs is highly necessary to identify effective treatments for patients with uncontrolled seizures.

The sigma-1 chaperone protein, also known as the sigma-1 receptor (Sig1R), in the cell plays a significant role in the modulation of the activity of endoplasmic reticulum-residing proteins, as well as nuclear, mitochondrial and plasma-membrane proteins, which are in close proximity to the endoplasmic reticulum (Mavlyutov et al., 2015; Su

* Corresponding author.
E-mail address: edijs.vavers@farm.osi.lv (E. Vavers).

https://doi.org/10.1016/j.nbd.2020.105244
Received 21 August 2020; Received in revised form 7 December 2020; Accepted 27 December 2020
Available online 30 December 2020
0969-9961/© 2020 The Author(s). Published by Elsevier Inc. This is an open access article under the CC BY-NC-ND license (http://creativecommons.org/licenses/by-nc-nd/4.0/).

et al., 2016). It has been shown that sigma ligands are involved in modulation of the seizure threshold, and both anti-convulsive and pro-convulsive activity has been observed for both agonists and antagonists (Vavers et al., 2017). Our previous data showed that the Sig1R antagonist NE-100 demonstrated pro-convulsive activity at a dose of 25 mg/kg after i.p. administration in a PTZ-induced seizure model, and after administration at doses of 50 and 75 mg/kg, NE-100 induced convulsions in naïve animals (Vavers et al., 2017). On the other hand, positive allosteric modulators of Sig1R clearly demonstrated anti-convulsive activity in in vivo seizure models (Guo et al., 2015; reviewed in Vavers et al., 2019). Taken together, these findings strongly suggest that Sig1R could be used as a novel drug target to treat seizures. The mechanism governing how Sig1R can control the balance between excitation and inhibition in vivo has not been fully elucidated. The first Sig1R knockout (Sig1R−/−) mice were described in 2003 (Langa et al., 2003), and to date, no spontaneous seizures have been observed in Sig1R−/− mice.

In several in vitro studies, it has been shown that Sig1R could alter neuronal excitability by modulating the function of voltage-gated sodium, potassium and calcium channels (Kourrich, 2017). The activation of Sig1R has been demonstrated to inhibit glutamate release in rat cerebral cortex nerve endings (Lu et al., 2012). On the other hand, it has been shown that endogenous activators and agonists of Sig1R, such as pregnenolone sulfate, dehydroepiandrosterone sulfate and (+)-pentazocine, can increase presynaptic glutamate release in rat hippocampal neurons (Meyer et al., 2002; Dong et al., 2007). In addition, pregnenolone sulfate and dehydroepiandrosterone sulfate have been demonstrated to negatively modulate and decrease the activity of the GABA-A receptor (Maurice et al., 2001) and thus may increase the sensitivity of mice to pentylenetetrazol (PTZ)-induced seizures (Reddy and Kulkarni, 1998). The lack of Sig1R in Sig1R−/− mice has been associated with dysfunction of GABA-A receptor-mediated inhibition in basolateral amygdala principal neurons, probably through the reduction of NMDA receptor-mediated GABA release (Zhang et al., 2017). A bidirectional modulation of Sig1R agonists of NMDA receptor evoked excitatory transmission, in which a low dose of Sig1R agonist is excitatory and a high dose is inhibitory (Liang and Wang, 1998), suggesting a complex mechanism that is responsible for regulating the balance between excitation and inhibition by Sig1R.

To determine the possible mechanisms governing the role of Sig1R in the control of seizures, the aim of this study was to compare the seizure threshold and behavioral response of WT and Sig1R−/− mice in different acute seizure models in vivo. Changes in seizure-related gene and protein expression were analyzed using PCR, Western blotting and immunohistochemistry techniques. The isolated *vasa deferentia* model was used to test the role of Sig1R in electrical current-induced contractility and potassium chloride-induced depolarization.

2. Materials and methods

2.1. Animals

In total, fifty WT (HSD:ICR(CD-1®), ENVIGO, Venray, Netherlands (https://www.envigo.com/model/hsd-icr-cd-1-)) and fifty age-matched CD-1 background Sig1R−/− (ENVIGO, Bresso, Italy) male mice aged 22–25 weeks were used in this study. Briefly, CD-1 background Sig1R−/− mouse model is a global knockout generated by homologous recombination techniques (Langa et al., 2003). Homologous recombination vector *pHR53TK* was constructed and used to inactivate the mouse Sig1R gene (GenBank: AF030199) in mouse embryonic stem cells (Langa et al., 2003). Fifteen and ten mice were employed in the PTZ- and BIC-induced seizure threshold tests, respectively. Nine mice per group (WT control, WT + NE-100, Sig1R−/− control and Sig1R−/− + NE-100) were used in the Sig1R antagonist NE-100-induced seizure model. Seven mice were used in the isolated *vasa deferentia* model. Three Wistar male rats (12 weeks; RccHan:WIST, ENVIGO, Venray, Netherlands (https://www.envigo.com/model/rcchan-wist)) were used for the [^{3}H] muscimol binding assay. All animals were housed under standard conditions (21–23 °C, 12 h light-dark cycle) with unlimited access to standard food (Lactamin AB, Mjölby, Sweden) and water in an individually ventilated cage housing system (Allentown Inc., Allentown, New Jersey, USA). Each cage contained bedding consisting of EcoPure™ Shavings wood chips (Datesand, Cheshire, UK), nesting material and a wooden block from TAPVEI (TAPVEI, Paekna, Estonia). For enrichment, transparent tinted (red) nontoxic durable polycarbonate Safe Harbor Mouse Retreat (Animalab, Poznan, Poland) was used. For the rat cage enrichment, nontoxic durable transparent polycarbonate rat retreats tinted red were used. The mice were housed at a density of 3 to 5 mice per standard cage (38 × 19 × 13 cm). The rats were housed at a density of 3 rats per standard cage (30 × 41 × 23 cm). All studies involving animals were reported in accordance with the ARRIVE guidelines (Kilkenny et al., 2010; McGrath et al., 2010). The experimental procedures were performed in accordance with the guidelines reported in EU Directive 2010/63/EU and in accordance with local laws and policies; all of the procedures were approved by the Latvian Animal Protection Ethics Committee of Food and Veterinary Service in Riga, Latvia. All experiments were performed by experienced scientists who were blinded to the experimental groups.

2.2. Intravenous PTZ- and BIC-induced seizure threshold tests

Chemoconvulsant-induced clonic and tonic seizures were initiated by inserting a 27-gauge needle into the tail veins and infusing 1% PTZ (Mandhane et al., 2007; Zvejniece et al., 2010) or 0.01% BIC (Meldrum, 1975; Vavers et al., 2017) at a constant rate of 20 μl/2 s to restrained animals. The infusion was halted when forelimb clonus followed by tonic seizures of the full body were observed. Minimal doses of PTZ or BIC (mg/kg of mouse weight) necessary to induce clonic and tonic seizures were considered as indices of seizure threshold. In BIC-induced seizure model one animal from WT control group was excluded from the data due to technical problems.

2.3. Sig1R antagonist NE-100-induced seizure model

Based on previous results (Vavers et al., 2017), this model was chosen to confirm the role of Sig1R in seizure modulation. NE-100-induced seizures were studied at a dose of 75 mg/kg, which induced seizures in 100% of animals (Vavers et al., 2017). NE-100 was injected intraperitoneally (i.p.), and mice were subsequently placed immediately in observation chambers (40 × 25 × 15 cm) and video-recorded for 60 min using a digital HD video camera recorder (Handycam HDR-CX11E, Sony Corporation, Tokyo, Japan). The scoring scale for observed behavioral responses of animals was adapted from a previously published seizure rating scale (Lüttjohann et al., 2009). Behavioral responses of animals were scored from the video files using the following scale: 0, no abnormality; 1, trembling or wobbly gait; 2, tail lifting; 3, clonic seizures while lying on belly; 4, tonic seizures while lying on belly; 5 clonic-tonic seizures while lying on belly; 6, motionless or sleeping; 7, clonic seizures while lying on side; 8, tonic seizures while lying on side; 9, clonic-tonic seizures while lying on side; 10, generalized seizures with wild jumping and running (Vavers et al., 2017). The maximal score was given for each 60-s period. The latency time until the first occurrence of seizures induced by NE-100 was also determined from the video files.

2.4. Quantitative PCR

Brain tissues were collected immediately after the decapitation of animals 75 min after i.p. administration of saline or NE-100 at a dose of 75 mg/kg. Both hemispheres of mouse brains were separated on ice and snap-frozen in liquid nitrogen. Brain samples were stored at −80 °C until isolation of RNA. Total RNA was isolated from the brain hemisphere

using an RNA Mini Kit (Life Technologies, Grand Island, New York, USA) according to the manufacturer's instructions. The extracted RNA was dissolved in 50 μl nuclease-free distilled water and stored at −80 °C until it was used for analysis. First-strand cDNA was synthesized using a High-Capacity cDNA Reverse Transcription Kit (Thermo Fisher Scientific, Waltham, MA, USA) following the manufacturer's protocol. Quantitative PCR analysis for Sig1R, sigma-2 receptor (Sig2R), glutamate ionotropic receptor NMDA type subunit 1, dopamine receptor 1 (D1R), dopamine receptor 2 (D2R), inducible nitric oxide synthase (iNOS), GABA-Aα5, GABA-Aβ3, GABA-Aγ2, GABA-B R1, GABA-B R2, binding immunoglobulin protein (BiP), P2X purinoceptor 1 (P2RX1), ryanodine receptor 3 (RyR3), inward rectifier potassium channel (Kcnj) 3 and Kcnj9, ionized calcium-binding adapter molecule 1 (Iba1), CD68 protein and beta-actin (β-actin) was performed using SYBR® Green Master Mix (Life Technologies, Grand Island, New York, USA). The primer sequences used in this study are presented in Supplementary Table 1. The primers were obtained from Metabion, Germany. The relative expression levels for each gene were calculated with the ΔΔCt method, normalized to the expression of β-actin and compared to the expression levels of age-matched WT animals.

2.5. Western blot analysis

The brain hemisphere was homogenized using Bead Ruptor (Omni International, USA) in urea buffer (4 mM urea, 140 mM Tris, 1% SDS, 10 mM EDTA, 5 mM $MgCl_2$, 1% IGEPAL, 1 mM AEBSF, 1 μg/mL aprotinin, 1 μM leupeptin, 1 μM pepstatin A, 1 mM DTT; pH = 7.4). The homogenization cycle was set to 30 s, 4 ms, 0.1 Hz. Homogenates were subsequently centrifuged at 10000 xg for 5 min at 4 °C and stored at −80 °C until use. The protein concentration in the sample was determined by the Lowry method (Lowry et al., 1951). Samples (22.5 μg of total protein) were loaded in the Invitrogen™ Bolt™ 4–12% Bis-Tris Plus Gel 12-well (Thermo Fisher Scientific, Waltham, MA, USA). SuperSignal™ Molecular Weight Protein Ladder (Thermo Fisher Scientific, Waltham, MA, USA) was utilized as a protein size marker. Electrophoresis was performed using a MES running buffer (50 mM MES, 50 mM TRIS, 0.1% SDS, 1 mM EDTA, pH = 7.24), and the conditions of 145 V, 1.0 A and 300 W were set on Mini Gel Tank (Thermo Fisher Scientific, Waltham, MA, USA). Proteins were transferred using Invitrogen™ iBlot™ 2 Transfer Stack PVDF membranes (Thermo Fisher Scientific, Waltham, MA, USA) on an Invitrogen™ iBlot™ 2 Dry Blotting System (Thermo Fisher Scientific, Waltham, MA, USA). After the transfer step, membranes were blocked in 5% BSA for 1 h and incubated with primary anti-GABA A receptor gamma 2/GABRG2 antibody (Cat# ab87328, Abcam, Cambridge, MA, USA) overnight at 4 °C. The following day, membranes were washed 6 times with TBS buffer and incubated with secondary anti-mouse IgG HRP-linked antibody (Cat# 7076, CST, Danvers, MA, USA) for 1 h at room temperature following repeated washing with TBS buffer. Images were captured using Immobilon Western Chemiluminescent HRP Substrate (Cat# WBKLS0500, Merck, Burlington, MA, USA) with an Azure c400 Visible Fluorescent Western Blot Imaging System (Azure Biosystems, Sierra Court, CA, USA). After imaging, membranes were blocked in 5% BSA and washed with TBS buffer, and the same membranes were used to detect the amount of the R2 subunit of the GABA-B receptor. The same protocol was applied to detect the GABA-B receptor using an anti-GABA-B receptor 2/GABBR2 antibody [EP2411Y] (Cat# ab75838, Abcam, Cambridge, MA, USA) and a secondary anti-rabbit IgG HRP-linked antibody (Cat# 7074, CST, Danvers, MA, USA). Images were quantified using AzureSpot 2.0 software (Azure Biosystems, Sierra Court, CA, USA).

2.6. [^{3}H]Muscimol binding assay

Membranes were isolated as described previously (Gould et al., 1995). Membrane fraction aliquots were thawed and diluted with 50 mM TRIS-citrate (pH = 7.1, +4 °C). The binding assay buffer consisted of 160 μl membrane aliquots (the final protein concentration was 30 μg/well), 20 μl of the test compound or deionized water containing DMSO for the control (final concentration of DMSO was 1%), and 20 μl [^{3}H] muscimol. The final concentration of [^{3}H]muscimol was 2 nM. Nonspecific binding was assessed by adding GABA (100 μM). The samples were incubated for 30 min on ice. The bound and free radioligands were separated by rapid filtration under vacuum (Harvester for 96-well microplates, Connectorate AG, Dieticon, Switzerland) using Millipore GF/B filter paper (Merck Millipore, Billerica, Massachusetts, USA). The filters were washed five times with ice cold 25 mM TRIS-citrate (pH = 7.1, +4 °C). The samples' radioactivity was measured with a Wallac MicroBeta2 liquid scintillation counter (PerkinElmer, Waltham, Massachusetts, USA).

2.7. Immunohistochemistry

Mice were anaesthetized using i.p. administration of ketamine (200 mg/kg) and xylazine (15 mg/kg). The depth of anesthesia was monitored by toe pinch. Animals were transcardially perfused at a speed of 3 ml/min with 0.01 M phosphate-buffered saline (PBS, pH = 7.4) for 5 min until the blood was completely removed from the tissue. After perfusion, brains were carefully dissected and fixed in 4% PFA overnight at 4 °C. Brains were cryoprotected with a 10–20-30% sucrose gradient over 72 h. Coronal sections (20 μm) were cut using a Leica CM1850 cryostat (Leica Biosystems, Buffalo Grove, IL, United States).

2.7.1. Cresyl violet staining

For cresyl violet staining, coronal frozen sections of mouse brain were used. Slides with sections on Superfrost Plus microscope slides (Thermo Scientific, Waltham, MA, United States) were rinsed in distilled water and then incubated with cresyl echt violet (Abcam; Cat# ab246817) for 5 min. Sections were quickly rinsed in distilled water, dried overnight at 37 °C, cleared in xylene and mounted using DPX mounting medium (Sigma-Aldrich, St. Louis, MO, United States) and finally coverslipped. Images were taken with a Nikon Eclipse TE300 microscope (Nikon Instruments, Tokyo, Japan).

2.7.2. Immunoperoxidase and immunofluorescence of free-floating sections

The staining of free-floating sections was performed based on a method described previously (Kadish et al., 2016) with slight modifications. Free-floating sections were pretreated for 30 min in 85 °C sodium citrate solution (pH = 6.0), for 15 min in 0.3% H_2O_2 (to block endogenous peroxidase), and for 15 min in 5% BSA (to block nonspecific background staining). Between each step, the sections were washed three times (5 min each) in TRIS-buffered saline containing Triton™ X-100 (TBS-T) and incubated for 16 h in TBS-T with a primary antibody. After incubation with primary antibody, sections were washed three times (5 min each) in TBS-T. For co-labeling experiments, the last two steps were repeated. Sections were subsequently incubated for 2 h at room temperature with a corresponding secondary antibody. The sections were washed three times (5 min each) in TBS-T. The following primary antibodies were used in this study: mouse anti-GABA-B R1 (1:2000, Abcam, Cat# ab55051), rabbit anti-GABA-B R2 (1:500 (for co-labeling staining) 1:2000 (for DAB staining), Abcam, Cat# ab75838), rabbit anti-GABA-A γ2 (1:1000, Abcam, Cat# ab87328), mouse anti-Substance P (1:200, R&D systems, Cat# MAB4375), mouse anti-choline acetyltransferase (ChAT, 1:200, Sigma-Aldrich, Cat# AMAB91129-25UL). The following secondary antibodies were used in this study: goat anti-mouse IgG (H + L) secondary antibody (1:1000, Invitrogen Cat# 31800), goat anti-rabbit IgG (H + L) secondary antibody (1:1000, Invitrogen Cat# 65–6140), goat anti-rabbit IgG H&L Alexa Fluor® 488 (1:200, Abcam, Cat# ab150077), goat anti-mouse IgG (H + L) Rhodamine Red-X (1:200, Invitrogen, Cat# R-6393), goat anti-mouse Abberior STAR GREEN (1:200, a gift from Abberior Instruments), goat anti-rabbit Abberior STAR RED (1:200, a gift from Abberior Instruments). Biotinylated antibodies were subsequently incubated for 2 h

at room temperature with streptavidin (HRP) (1:1000, Abcam Cat# ab7403). Again, the sections were washed three times (5 min each) in TBS-T and incubated with freshly prepared DAB reagent for 2 min at room temperature. DAB-stained sections were mounted on gelatinized slides, cleared in xylene, mounted using DPX mounting medium (Sigma-Aldrich, St. Louis, MO, United States), coverslipped, and finally photographed and measured. Fluorescently labeled sections were mounted using Abberior Mount solid antifade (a gift from Abberior Instruments).

2.7.3. Iba1 and GFAP staining

Immunohistochemistry was performed using a Rabbit Specific HRP/DAB (ABC) Detection IHC Kit (Abcam, Cat# ab64261) following the manufacturer's instructions. Slices were incubated with primary anti-Iba1 antibody (1:1000; Abcam, Cat# ab153696) or anti-GFAP antibody (1:1000, Abcam, Cat# ab7260) for 16 h at +4 °C. The antibodies were diluted in PBS containing 3% BSA and 0.3% Triton™ X-100. Stained sections were mounted using DPX mounting medium (Sigma-Aldrich, St. Louis, MO, United States) and coverslipped. Images were taken with a Nikon Eclipse TE300 microscope (Nikon Instruments, Tokyo, Japan).

2.7.4. Image analysis

Identical brain sections corresponding to identical anatomical structures were used for the analysis. The structures were validated using Allen Mouse Brain atlas (http://mouse.brain-map.org/static/atlas). For each antibody staining experiment, sections from all animals were processed in the same staining tray. Negative controls replacing the primary antibody with a buffer solution only (TBS-T) were performed. Obtained OD values of corresponding background staining were subtracted from the total OD values measured for each brain structure. In the quantification experiments, data were collected from 3 mice per genotype, each hemisphere was analyzed separately. In the co-labeling experiments, at least two mice and three sections per mouse were used for analysis. Images were taken with a Nikon Eclipse TE300 microscope (Nikon Instruments, Tokyo, Japan). Higher resolution images for co-labeling were collected using a Leica TCS SP8 confocal microscope (Leica Microsystems GmbH, Wetzlar, Germany) with a 60×-oil objective. Staining was quantified using ImageJ software (ImageJ v1.52a). Eight-bit images were generated from the pictures and were cropped to contain the regions of interest. Means of optical density (OD) were used to quantify the staining intensity of GABA-B R1 and R2 and GABA-A γ2 in specific brain structures. For optical density (OD) analysis, calibration was performed in accordance with the instructions on the ImageJ software website (https://imagej.nih.gov/ij/docs/examples/calibration/). Images for Iba1 and GFAP staining were thresholded to select a specific signal over the background, and the stained area for each region was calculated and employed for statistical analysis.

2.8. Electrical field stimulation-induced contractions of isolated vasa deferentia

Both *vasa deferentia* of WT and Sig1R−/− CD-1 mice were excised and immersed in a modified ice-cold Krebs-Henseleit buffer solution (content in mmol/l: NaCl 118.0, KCl 4.8, $CaCl_2$ 2.5, $NaHCO_3$ 24.9, K_2HPO_4 1.2, glucose 10.0 and EDTA 0.05, without $MgCl_2$). Cleaned whole *vas deferens* (~10 mm) were mounted in 10-ml organ baths and incubated in a modified Krebs-Henseleit buffer solution that was maintained at 32 °C and bubbled with 95% CO_2 and 5% O_2 (with the slight modifications described by Kennedy and Henderson, 1989). The passive tension was fixed at 0.5 g, and the buffer solution in the organ bath was changed every 15 min. After a 60-min adaptation period, the isolated *vasa deferentia* were stimulated with an electrical current set at 0.1 Hz, a pulse duration of 2 ms, and a voltage of 10 V (DMT CS8 stimulator, Hinnerup, Denmark). Baseline maximal contractility of the *vas deferens* was induced by the addition of 100 mM KCl. Next, the electrical stimulation was turned off, and each isolated *vasa deferentia* was washed several times with a modified Krebs-Henseleit buffer solution. After 30 min, electrical stimulation was resumed under the same parameters. When the stimulation produced a stable contraction amplitude, cumulative doses of the Sig1R antagonist NE-100 (at concentrations ranging from 1 to 10 μM) or barium chloride (at concentration ranging from 1 to 100 μM) were added. After reaching the plateau contraction amplitude, 100 mM KCl was added to induce maximal contraction. *Vas deferens* with contraction amplitude below the amplitude of 0.05 g at baseline was excluded from the experiment.

2.9. Chemicals

PTZ and BIC were purchased from Sigma-Aldrich Co. Louis, MO, USA). NE-100 (4-methoxy-3-(2-phenylethoxy)-N,N-dipropylbenzeneethanamine hydrochloride) was obtained from Tocris Bioscience (Bristol, UK). Physiological saline (0.9%) was purchased from Fresenius Kabi (Warszawa, Poland). [^{3}H]Muscimol (S.A. 30.2 Ci/mmol) was obtained from BIOTREND Chemikalien GmbH (Köln, Germany). PTZ was weighed and dissolved in 0.9% physiological saline to make a 1% PTZ solution. BIC was dissolved in DMSO to prepare a 1% stock solution, which was subsequently diluted with saline to make a 0.01% BIC solution. PTZ and BIC solutions were freshly prepared before each experiment. Compounds were dissolved in saline before use.

2.10. Experimental design and statistical analysis

2.10.1. Sample size calculations

Through a power calculation (using G-power software) for a *t*-test (two group comparison) with $\alpha = 0.05$, a power of 80%, and a standardized effect size Cohen's $d = 1.2$, a total sample size of 10 mice per group was deemed to be sufficient. In the BIC-induced seizure model, we used 10 mice per group. In the PTZ-induced seizure model, we used 15 mice per group due to higher variability in this model compared to the BIC-induced seizure model. Our sample size of $n = 15$ would also enable smaller differences to be identified with the same statistical power for the same significance level.

In the NE-100-induced seizure model, it was expected that the Sig1R antagonist NE-100 could not induce seizures in Sig1R−/− animals. Therefore, differences between WT and Sig1R−/− animals were expected to be highly pronounced. Through a power calculation for a two-way ANOVA test (four group comparison) with $\alpha = 0.05$, a power of 80%, and a standardized effect size Cohen's $f = 0.7$, a total sample size of 8 mice per group was determined to be sufficient. Since it was previously reported that NE-100 at a dose of 75 mg/kg could induce death in some animals (Vavers et al., 2017), an additional 1 animal was added to each group of NE-100-induced seizure models. Our sample size of $n = 9$ would also enable smaller differences to be identified with the same statistical power for the same significance level.

2.10.2. Statistical data analysis

The statistical calculations were performed using the GraphPad Prism software package (GraphPad Software, Inc., La Jolla, California, USA). For two-group comparisons, Student's *t*-test or Mann-Whitney *U* test were used for the datasets that were normally or not normally distributed, respectively. The Shapiro-Wilk test was used to test the distribution of the data. Time and genotype interactions in the NE-100-induced seizure model were analyzed by using repeated measures two-way ANOVA. Ordinary two-way ANOVA was used for the comparison of the WT control, Sig1R−/− control, WT + NE-100 and Sig1R−/− + NE-100 groups in the NE-100-induced seizure model. Repeated measures two-way ANOVA was used to compare the dose-dependent effect of NE-100 and barium chloride between WT and Sig1R−/− mice in an isolated *vasa deferentia* model. A post hoc test was performed if ANOVA indicated significant differences. *p* values less than 0.05 were considered to be significant.

3. Results

3.1. Sig1R−/− mice are more prone to PTZ- and BIC-induced tonic seizures

The susceptibility to seizures of WT and Sig1R−/− mice was compared in timed intravenous PTZ and BIC infusion-induced acute seizure models. The 1% PTZ intravenous infusion induced clonic and tonic seizures in WT animals at doses of 33 ± 1 mg/kg and 70 ± 6 mg/kg, respectively (Fig. 1A, B). Compared to WT mice, Sig1R−/− mice demonstrated clonic seizures at a dose of 31 ± 1 mg/kg of PTZ (Fig. 1A), while tonic seizures were observed at a dose of 50 ± 4 mg/kg of PTZ (Fig. 1B). The response of the PTZ-induced clonic seizures did not differ between WT and Sig1R−/− animals (Mann-Whitney *U* test: $p = 0.2328$; Fig. 1A). In Sig1R−/− mice, the PTZ-induced tonic seizure threshold was significantly decreased by 28% compared to WT animals (Mann-Whitney U test: $p = 0.0041$; Fig. 1B). BIC-induced clonic and tonic seizures in WT animals were observed at doses of 0.61 ± 0.03 mg/kg and 1.12 ± 0.09 mg/kg of BIC, respectively (Fig. 2A and B). The response of the BIC-induced clonic seizures did not differ between WT and Sig1R−/− animals (unpaired *t*-test: $t_{(17)} = 0.8$, $p = 0.4539$; Fig. 2A). Similar to the PTZ-induced seizure model, the tonic seizure threshold was significantly decreased in Sig1R−/− mice by 22% (0.88 ± 0.04 mg/kg of BIC; unpaired t-test: $t_{(17)} = 2.6$, $p = 0.0187$) compared to WT mice (Fig. 2B), thereby demonstrating that Sig1R−/− mice are more susceptible to tonic seizures in both PTZ- and BIC-induced seizure models.

3.2. Sig1R−/− mice demonstrate decreased severity of seizure in the NE-100-induced seizure model

The responses of WT and Sig1R−/− mice in the NE-100-induced seizure model were different and could be divided into two phases. Acute seizures of NE-100 (up to 20 min) were observed in both WT and Sig1R−/− mice, while the second phase, which started 20–22 min after administration of NE-100, was observed only in WT animals (Fig. 3A). The average maximal seizure score in WT mice was 7.6 while in Sig1R−/− mice it was 5.4 points (Fig. 3A). There was a significant genotype x time interaction observed between seizure severities (two-way repeated-measures ANOVA: $F_{(59,\ 944)} = 4.3$, $p < 0.0001$ for genotype x time interaction; $F_{(1,\ 16)} = 17.4$, $p = 0.0007$ for genotype; $F_{(5,\ 83)} = 19.2$, $p < 0.0001$ for time; Fig. 3A). As demonstrated by the data expressed as the areas under the curves (AUCs), the seizure severity after administration of NE-100 in Sig1R−/− mice was less pronounced than that in WT animals (Mann-Whitney *U* test: $p = 0.0040$; Fig. 3B). Compared to WT animals, in which seizures lasted at least 34 min (Fig. 3A, C), the NE-100-induced seizures in Sig1R−/− mice lasted for significantly shorter lengths of time (Mann-Whitney *U* test: $p = 0.0012$; Fig. 3C). One Sig1R−/− mouse did not show any signs of seizures after administration of NE-100 at a dose of 75 mg/kg (Fig. 3B, C). Sig1R−/− mice exhibited a significantly higher latency time to NE-100-induced seizures (Mann-Whitney *U* test: $p = 0.0380$; Fig. 3D). NE-100-induced clonic seizures in Sig1R−/− mice were observed for a significantly shorter time than in WT animals (Mann-Whitney *U* test: $p = 0.0199$ for clonic seizures while lying on the belly; $p = 0.0097$ for clonic seizures while lying on the side; Fig. 4).

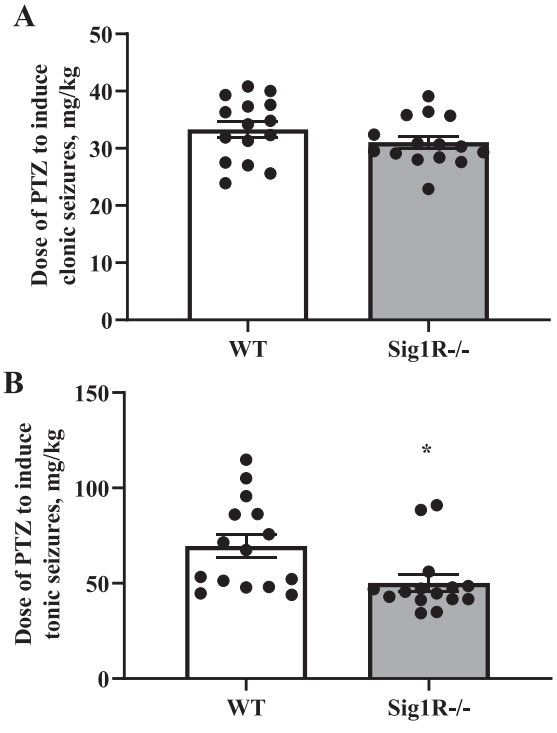

Fig. 1. Comparison of the response of WT and Sig1R−/− mice in the PTZ-induced seizure model. PTZ-induced clonic (A) and tonic (B) seizure thresholds. Data are expressed as the mean ± SEM ($n = 15$). *$p < 0.05$ Sig1R−/− mice vs WT mice (Mann-Whitney test).

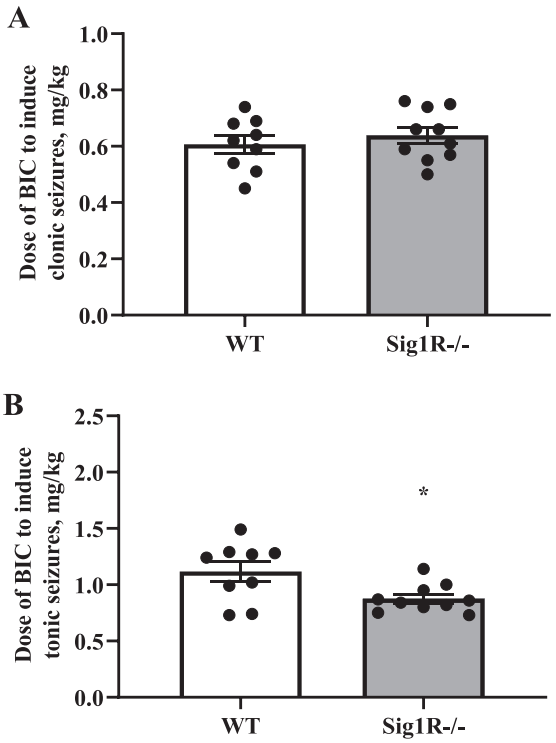

Fig. 2. Comparison of the response of WT and Sig1R−/− mice in the BIC-induced seizure model. BIC-induced clonic (A) and tonic (B) seizure thresholds. Data are expressed as the mean ± SEM ($n = 9$ WT mice and $n = 10$ Sig1R−/− mice). *$p < 0.05$ Sig1R−/− mice vs WT mice (unpaired t-test).

3.3. NE-100-induced seizures result in the downregulation of mRNA levels of iNOS and the γ2 subunit of the GABA-A receptor

Sig1R gene expression was observed only in WT mice, but not in Sig1R−/− mice (Table 1). No significant differences in other investigated gene expression levels were found between WT and Sig1R−/− control mice (Table 1). However, Sig1R−/− animals presented a slight tendency of decreased GABA-B R2 mRNA levels (Mann-Whitney *U* test: $p = 0.1111$; Table 1). The administration of NE-100 induced significant downregulation of the gene expression of iNOS (Mann-Whitney U test: $p = 0.0022$) and the γ2 subunit of the GABA-A receptor (Mann-Whitney U

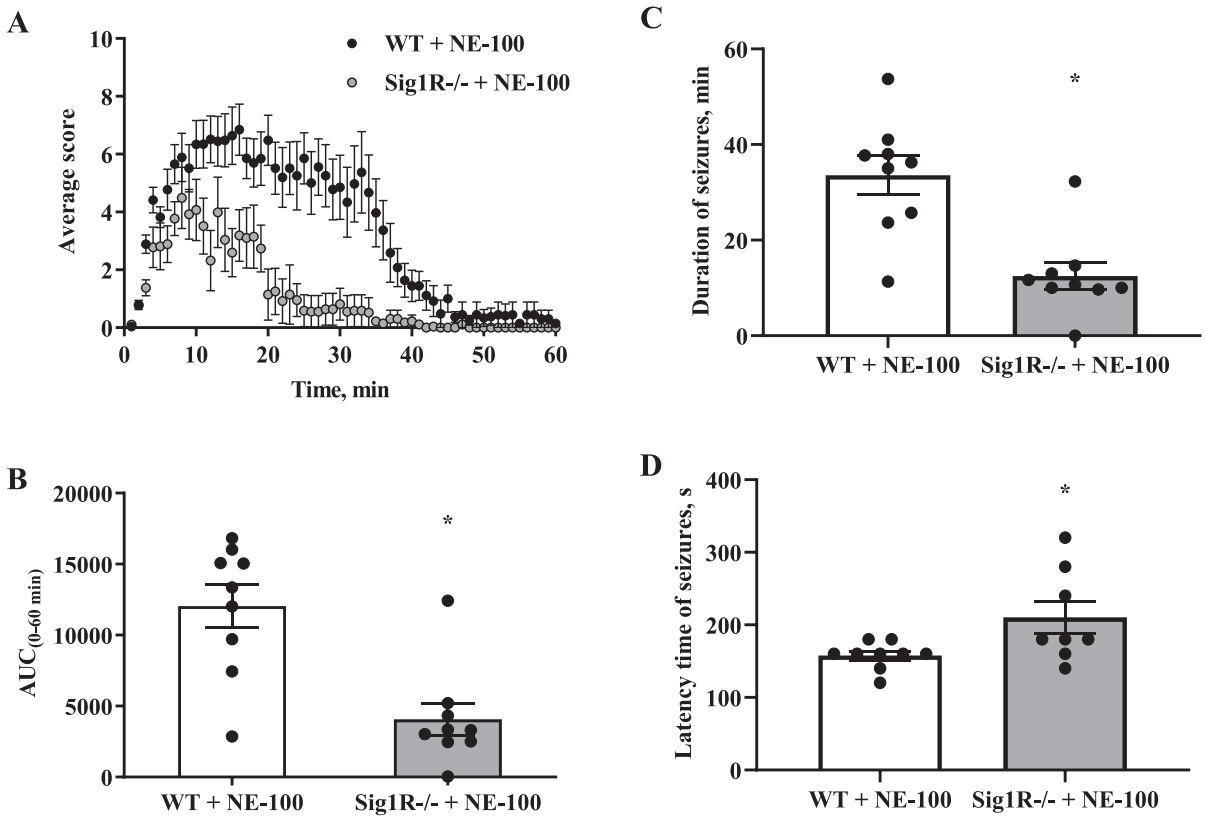

Fig. 3. NE-100-induced acute seizure model. (**A**) Average behavioral scores for each group during the 60-min observation period. Data are expressed as the mean for each 1 min period. (**B**) The area under the curve ($AUC_{0\text{-}60min}$) was calculated from the behavioral scoring curve. (**C**) Duration time of seizures for each animal and (**D**) latency time of NE-100-induced seizures. Data are expressed as the mean ± SEM ($n = 9$). *$p < 0.05$ Sig1R−/− mice vs WT mice (Mann-Whitney test).

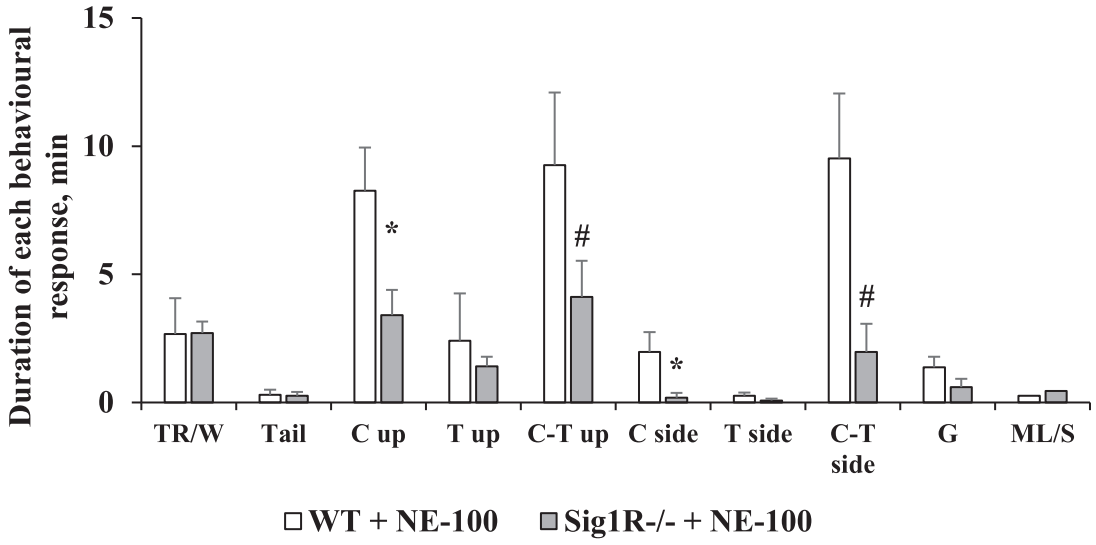

Fig. 4. Comparison of the duration of each observed seizure behavior after administration of NE-100 in WT and Sig1R−/− mice. The different behavioral categories include: trembling or wobbly gait (TR/W), tail lifting (Tail), clonic, tonic and clonic-tonic seizures while lying on the belly (C, T and C-T up, respectively), clonic, tonic and clonic-tonic seizures while lying on the side (C, T and C-T side, respectively), generalized seizures with wild jumping and running (G), and motionless or sleeping (ML/S). Data are expressed as the mean ± SEM (n = 9). *$p < 0.05$ and $^{\#}p = 0.06$ Sig1R−/− mice vs WT mice (Mann-Whitney test).

test: $p = 0.0303$) in WT mice (Table 1). Significant downregulation of the gene expression of iNOS (Mann-Whitney U test: $p = 0.0159$) and the γ2 subunit of the GABA-A receptor (Mann-Whitney U test: $p = 0.0286$) was also observed in Sig1R−/− mice after administration of NE-100 (Table 1).

3.4. Sig1R−/− mice demonstrate reduced expression of the R2 subunit of the GABA-B receptor

Based on gene expression data, we attempted to evaluate the protein expression levels of the R2 subunit of the GABA-B receptor and the γ2 subunit of the GABA-A receptor in the brain between WT and Sig1R−/−

Table 1
Gene expression.

Genes	Protein	Gene expression, fold change vs WT		
		Sig1R−/−	WT +NE-100	Sig1R−/− +NE-100
Sigmar1	Sig1R	–	0.8 ± 0.2	–
Pgrmc1	Sig2R	1.1 ± 0.6	1.0 ± 0.2	0.9 ± 0.1
Grin1	NMDAR1	1.0 ± 0.3	0.9 ± 0.3	0.8 ± 0.2
Drd1	D1R	0.8 ± 0.4	1.1 ± 0.8	1.0 ± 0.5
Drd2	D2R	0.8 ± 0.5	1.0 ± 0.8	1.0 ± 0.6
Nos2	iNOS	1.0 ± 0.5	**0.5 ± 0.2** ↓*	**0.5 ± 0.1** ↓*
Gabra5	GABA-A α5	1.0 ± 0.8	1.1 ± 0.3	0.8 ± 0.2
Gabrb3	GABA-A β3	1.1 ± 0.6	0.9 ± 0.2	0.8 ± 0.1
Gabrg2	GABA-A γ2	0.9 ± 0.7	**0.4 ± 0.4** ↓*	**0.5 ± 0.3** ↓*
Gabbr1	GABA-B R1	0.9 ± 0.1	0.9 ± 0.3	0.9 ± 0.2
Gabbr2	GABA-B R2	**0.6 ± 0.3** ↓	1.3 ± 0.6	1.2 ± 0.3
HSPA5	BiP	0.9 ± 0.2	1.1 ± 0.4	0.8 ± 0.4
P2rx1	P2RX1	0.7 ± 0.5	0.7 ± 0.4	1.1 ± 0.3
Ryr3	RyR3	0.9 ± 0.2	1.1 ± 0.6	0.7 ± 0.2
Kcnj3	$K_{ir}3.1$	0.8 ± 0.1	0.9 ± 0.4	1.0 ± 0.6
Kcnj9	$K_{ir}3.3$	0.7 ± 0.1	**0.6 ± 0.3** ↓	0.8 ± 0.3
Aif1	Iba1	1.1 ± 0.4	1.3 ± 0.8	1.0 ± 0.3
Cd68	CD68	1.2 ± 0.6	1.1 ± 0.1	0.8 ± 0.2

The relative expression levels for each gene were calculated with the ΔΔCt method, normalized to the expression level of β-actin and compared to the expression levels of WT control mice. Data are expressed as the mean fold change ± SD. *$p < 0.05$ NE-100 vs respective genotype control ($n = 5$; Mann-Whitney *U* test).

mice by using Western blot analysis. Sig1R−/− mice demonstrated significantly decreased expression of the GABA-B receptor R2 subtype compared to WT mice (Fig. 5A and B). The results showed no significant differences in the expression of the γ2 subunit of the GABA-A receptor between WT and Sig1R−/− animals (Fig. 5A and C). Although NE-100 induced a significant downregulation of the expression of the γ2 subunit of the GABA-A receptor, no difference in protein levels was observed in WT mice (Supplementary Fig. 1A and Supplementary Fig. 1B) and Sig1R−/− mice (Supplementary Fig. 1C and Supplementary Fig. 1D) after administration of NE-100. In addition, NE-100 was not observed to bind directly to the GABA-A receptor in the [^{3}H]muscimol binding assay (Supplementary Fig. 2).

To test which brain regions have decreased expression of the GABA-B receptor in Sig1R−/− mice, immunohistochemical staining of both the R1 and R2 subunits of the GABA-B receptor was performed (Fig. 5D, E and I). Sig1R−/− mice demonstrated significantly increased staining of GABA-B R1 in the *stratum oriens* (Mann-Whitney *U* test: $p = 0.0043$) and *stratum radiatum* (Mann-Whitney U test: $p = 0.0260$) while reduced staining of GABA-B R2 was observed in the *stratum oriens* (Mann-Whitney U test: $p = 0.0108$), *stratum radiatum* (Mann-Whitney U test: $p = 0.0087$) and *stratum lacunosum-moleculare* (Mann-Whitney U test: $p = 0.0022$) of the hippocampal *Cornu Ammonis* 1 (CA1) region (Fig. 5G). The most marked difference in the staining of the R2 subunit of the GABA-B receptor in Sig1R −/− mice was found in the habenula (Fig. 5I). The expression of the R2 subunit of the GABA-B receptor was significantly decreased in the Sig1R −/− mice medial and lateral habenula (Mann-Whitney *U* test: $p = 0.0022$ and $p = 0.0476$, respectively; Fig. 5K). Immunofluorescence staining of the GABA-B R2 in the medial habenula confirmed DAB staining results (Mann-Whitney U test: $p = 0.0022$; Fig. 6A and B). By using co-labeling experiments the most significant decrease of the R2 staining of the GABA-B receptor in Sig1R−/− mice was found in the ventral part of the medial habenula (Fig. 6C and D) and was confirmed with confocal imaging (Fig. 6E). GABA-B R1 staining in the habenula did not differ between WT and Sig1R−/− animals (Fig. 5J and Fig. 6E). Administration of NE-100 did not change the GABA-B R2 protein levels in the hippocampus (Supplementary Table 2) and habenula (Supplementary Fig. 4A and 4B) of WT and Sig1R−/− mice. We did not observe any significant difference in the staining of the γ2 subunit of the GABA-A receptor in the brain between WT and Sig1R−/− mice (Fig. 5E, H, I and L).

3.5. NE-100 enhances electrically stimulated contractions of isolated vasa deferentia and inhibits KCl-induced maximal contractility

The isolated *vasa deferentia* model has been used previously to test and describe the activity of Sig1R ligands. The activity of NE-100 on electrical field stimulation-induced contractions of isolated *vasa deferentia* of WT and Sig1R−/− mice was investigated. NE-100 dose-dependently enhanced electrical current-induced contractions of the *vasa deferentia* of WT and Sig1R −/− mice (Fig. 7A). A two-way repeated measures ANOVA showed a significant interaction between concentration of NE-100 and genotype ($F_{(3,33)} = 43.9$, $p < 0.0001$) and main effects of concentration of NE-100 ($F_{(1,\ 16)} = 98.6$, $p < 0.0001$) and genotype ($F_{(1,11)} = 17.8$, $p = 0.0015$; Fig. 7A). The contractions of *vasa deferentia* were significantly higher in WT than in Sig1R−/− mice after treatment with NE-100 at concentrations of 3 and 10 μM (two-way repeated measures ANOVA followed by Bonferroni test: $p < 0.0001$ and $p < 0.0001$, respectively; Fig. 7A). NE-100 significantly inhibited the response of *vasa deferentia* to KCl in both WT and Sig1R−/− animals (one-way ANOVA: $F_{(3,22)} = 56.7$, $p < 0.0001$; Fig. 7B). Compared to WT mice, Sig1R−/− mice demonstrated decreased maximal contractility of *vasa deferentia*, which was measured by the addition of 100 mM KCl (one-way ANOVA followed by Tukey's test: $p = 0.0011$; Fig. 7B). We examined the dose-dependent activity of barium chloride, a nonspecific inhibitor of inward-rectifier potassium channels, on the contractility of *vasa deferentia* isolated from WT and Sig1R−/− animals (Fig. 7C). Barium chloride dose-dependently enhanced electrical current-induced contractions of both genotype *vasa deferentia* (two-way repeated-measures ANOVA: $F_{(5,\ 50)} = 179.3$, $p < 0.0001$ for concentration of barium chloride; Fig. 7C). The effect of barium chloride was significantly less pronounced on *vasa deferentia* isolated from Sig1R−/− mice (two-way repeated measures ANOVA: $F_{(5,\ 50)} = 10.1$, $p < 0.0001$ for concentration of barium chloride and genotype interaction; Fig. 7C).

4. Discussion

This study demonstrates a reduced tonic seizure threshold of Sig1R−/− animals in PTZ and BIC-induced acute seizure models and decreased expression of the R2 subunit of the GABA-B receptor in the ventral part of the medial habenula and CA1 region of hippocampus compared to that of age-matched WT mice. NE-100-induced seizure severity was significantly less pronounced in Sig1R−/− mice. Sig1R-independent downregulation of gene expression of iNOS and GABA-Aγ2 in the brain was observed 75 min after the administration of NE-100. Sig1R−/− animals showed a reduced response to KCl, which resulted in decreased maximal contractility of *vasa deferentia* compared to WT animals. NE-100 inhibited KCl-induced depolarization of the *vasa deferentia* in both WT and Sig1R−/− mice.

Since Sig1R−/− mice previously exhibited dysfunction of GABA-A receptor-mediated inhibition (Zhang et al., 2017), to compare the seizure threshold in WT and Sig1R−/− animals, we used PTZ and BIC, which both inhibit the GABA-A receptor and induce seizures in naïve animals (Galanopoulou and Moshé, 2014). Our results showed that Sig1R−/− mice are more vulnerable to PTZ- and BIC-induced tonic seizures. To date, direct protein-protein interactions of Sig1R with the GABA receptors have not been demonstrated. Previously, the analysis of RT-PCR samples from C57Bl/6 background mice showed that the levels of GABA-Aα4 and GABA-Aδ mRNA in brain samples from the basolateral amygdala did not differ significantly between Sig1R−/− and WT mice (Zhang et al., 2017). In addition, we did not find differences in GABA-Aα5, GABA-Aβ3 and GABA-Aγ2 mRNA levels in CD-1 background Sig1R−/− mouse brain samples. Western blotting results showed that the γ2 subunit of GABA-A receptor expression in brain samples was not altered in Sig1R−/− mice compared to WT animals. It was reported previously that the direct function of the GABA-A receptor in

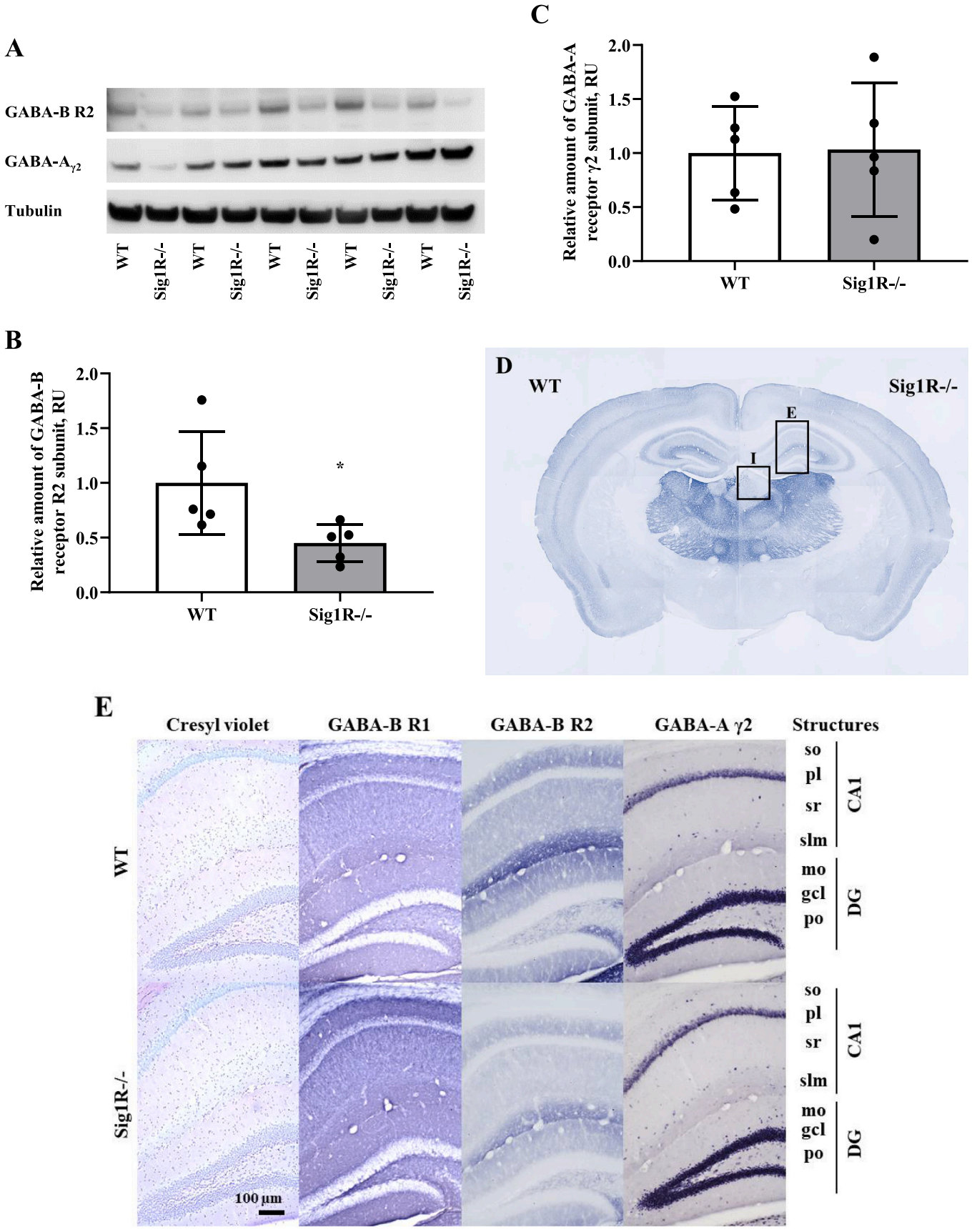

Fig. 5. GABA-A and GABA-B receptor expression in WT and Sig1R−/− mouse brains. Western blot images (**A**) and calculated relative amounts of the R2 subunit of the GABA-B (**B**) and γ2 subunit of the GABA-A (**C**) receptors of WT vs Sig1R−/− control animals. Data are expressed as the mean ± SD ($n = 5$). *$p < 0.05$ Sig1R−/− mice vs WT mice (Mann-Whitney U test). Overview of GABA-B R2 staining in WT (on the left) and Sig1R−/− (on the right) mouse brain hemispheres (**D**) with the

indicated areas used for analysis. Representative images of immunohistochemical staining in the hippocampus (**E**) and habenula (**I**). Measured optical density (OD) of the staining intensity of the GABA-B R1 in the hippocampus (**F**), and habenula (**J**), GABA-B R2 in the hippocampus (**G**) and habenula (**K**) and GABA-A γ2 in the hippocampus (**H**) and habenula (**L**). Data are expressed as the mean ± SD ($n = 6$). *$p < 0.05$ Sig1R−/− mice vs WT mice (Mann-Whitney U test). *Cornu Ammonis 1* (CA1), *dentate gyrus* (DG), *stratum oriens* (so), *pyramidal layer* (pl), *stratum radiatum* (sr), *stratum lacunosum-moleculare* (slm), *molecular layer* (mo), *granule cell layer* (gcl), *polymorph layer* (po), medial habenula (MHb) and lateral habenula (LHb).

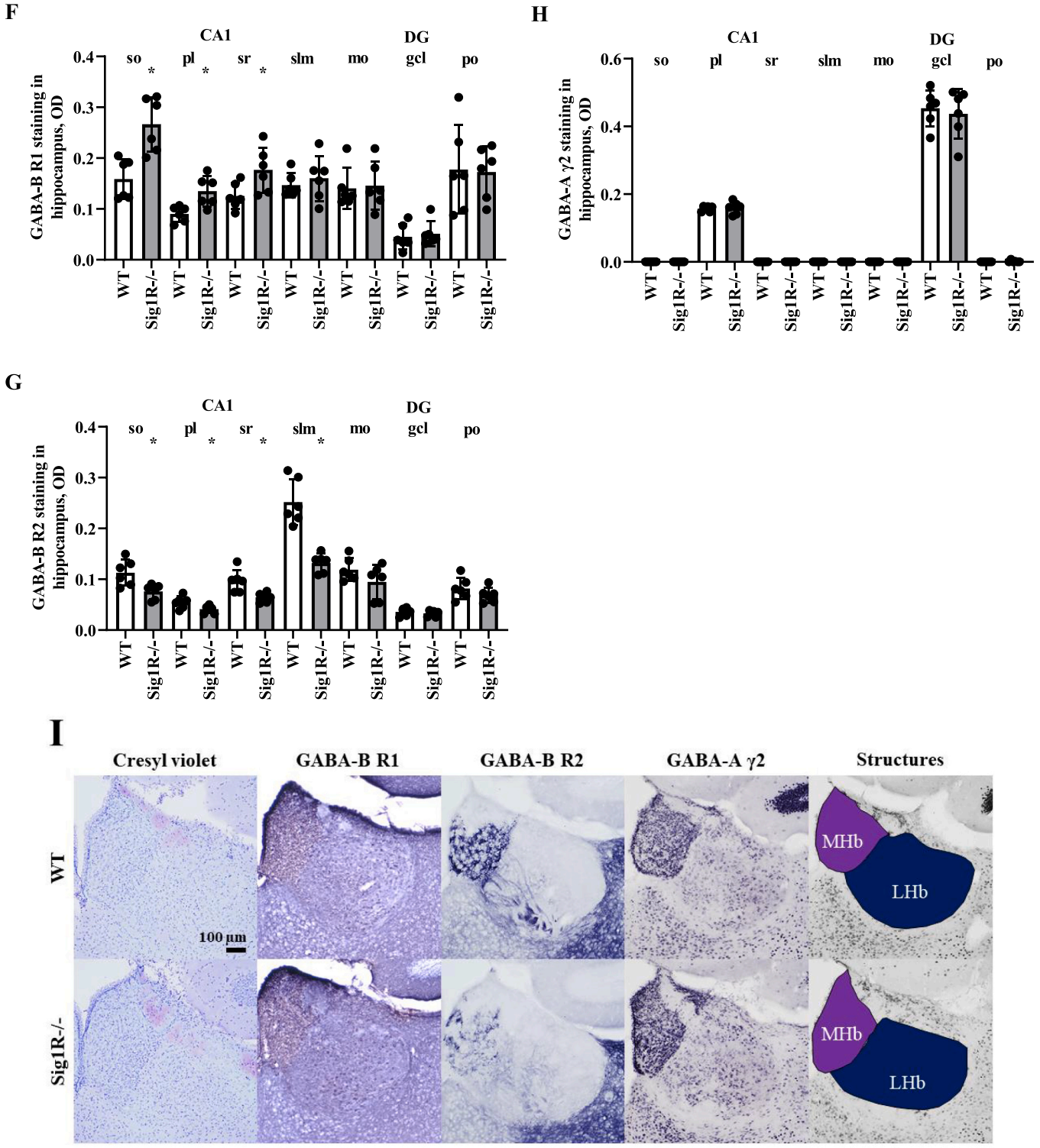

Fig. 5. (*continued*).

hippocampal pyramidal neurons of Sig1R−/− mice is not changed (Sha et al., 2013). Therefore, different seizure thresholds in PTZ- and BIC-induced seizure models could not be associated with different amounts or functions of the GABA-A receptor in CD-1 background WT and Sig1R−/− mice.

In our study, we demonstrated significantly decreased expression of

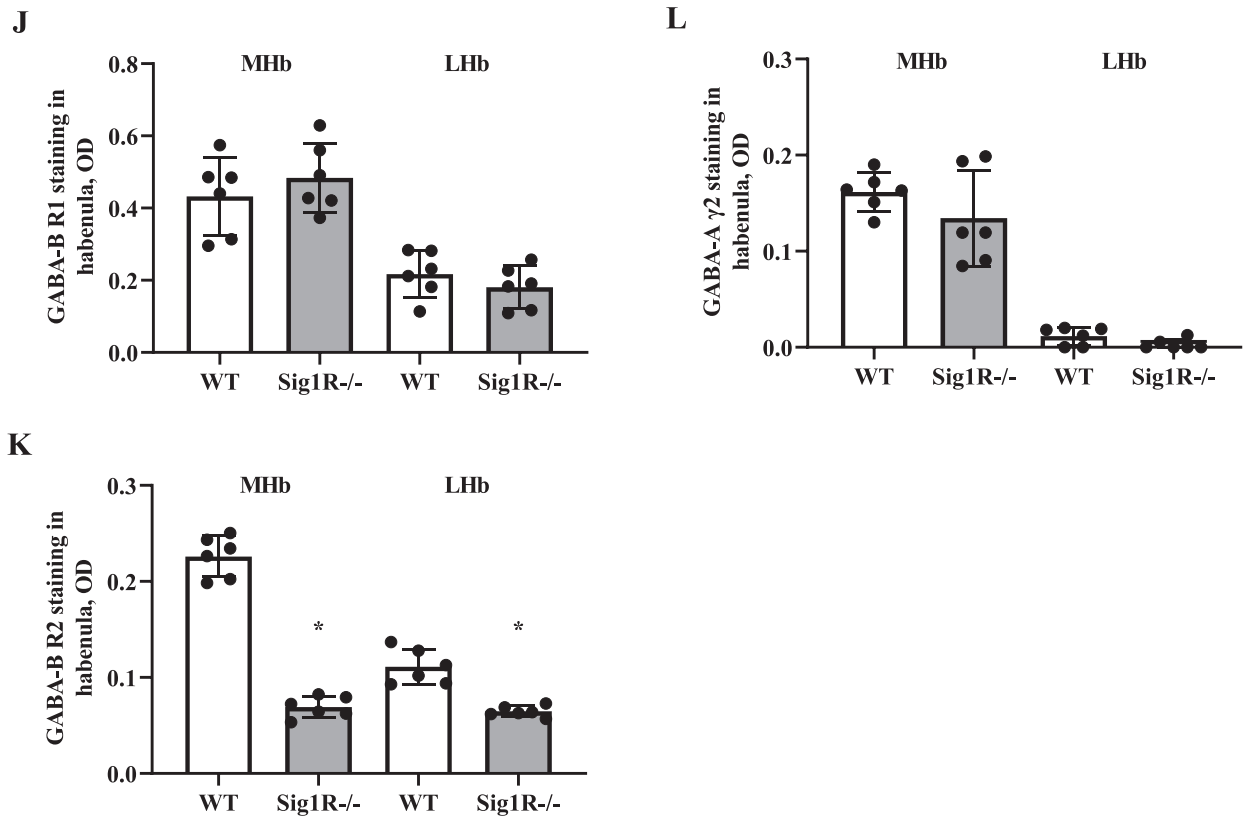

Fig. 5. (*continued*).

the R2 subunit of the GABA-B receptor in the habenula and hippocampus of Sig1R−/− mouse brain tissue. We found significantly increased expression of R1 subunit of GABA-B receptors in the CA1 region of the hippocampus of Sig1R−/− mice. This could be considered as a compensatory mechanism in Sig1R−/− animals due to decreased expression of the R2 subunit of the GABA-B receptor in the structures of CA1. Altered GABA-B receptor function has been associated with a variety of neurological and psychiatric disorders, including epilepsy, depression, anxiety, cognition, nociception and drug addiction (reviewed in Han et al., 2013; Felice et al., 2016; Terunuma, 2018), and Sig1R has been established as a molecular target to treat the above-mentioned disorders (Maurice and Su, 2009; Vavers et al., 2019). In addition, it has been demonstrated that the medial habenula plays an important role in stress, depression, memory and addiction (Viswanath et al., 2014). Functional GABA-B receptors are heterodimers whose function depends on the dimerization of the GABA-B R1 and GABA-B R2 subunits (reviewed in Bowery et al., 2002; Frangaj and Fan, 2018). It has been shown that mice lacking either the R1 or R2 subunit of the GABA-B receptor demonstrate altered anxiety and depression-related behavior (Mombereau et al., 2005), which is associated with behavioral changes found in C57Bl/6 background Sig1R−/− mice (Sabino et al., 2009; Chevallier et al., 2011; Couly et al., 2020). In addition, spontaneous seizures have been observed in GABA-B R2 subunit knockout mice (Mombereau et al., 2005). The medial habenula is divided into two subnuclei on the basis of cell type: cholinergic neurons are located in the ventral part of the medial habenula while Substance P-ergic neurons are located exclusively in the dorsal part of the medial habenula (Lee et al., 2019). By using Substance P and ChAT as markers of the dorsal and ventral parts of the medial habenula, respectively, we demonstrated that the decrease of the R2 subunit of the GABA-B receptor in Sig1R−/− mice is present in the ventral part of the medial habenula. In the brain, the medial habenula contains one of the highest concentrations of GABA-B receptors, suggesting the presence of strong inhibitory inputs (Viswanath et al., 2014). Presynaptic GABA-B receptors are abundant in cholinergic neurons of the medial habenula and control not only the release of acetylcholine but also glutamate (Lee et al., 2019). The reduced expression of the GABA-B receptor R2 subunit and disturbed GABA-B receptor function may explain the neurobehavioral phenotype of Sig1R−/− mouse and higher susceptibility to seizures.

GABA-B receptor agonists have been shown to diminish seizure activity in mouse models of both generalized convulsive and focal seizures (Joshi et al., 2016). Activation of GABA-B receptors with R-baclofen dose-dependently attenuated PTZ-induced kindling in CD-1 mice, while inhibition of GABA-B receptor by antagonists CGP 35348 and CGP 55845 resulted in more rapid development of kindling in the same model (De Sarro et al., 2000). It has been shown that activation of the GABA-B receptor in rat *globus pallidus* can reduce PTZ-induced tonic seizures (Chen et al., 2004). In patients with temporal lobe epilepsy significantly decreased number of GABA-B receptor binding sites were observed in the hippocampus (Furtinger et al., 2003). Taken together, these findings suggest that the reduced expression of the GABA-B receptor could explain why Sig1R−/− mice demonstrate a significantly increased susceptibility to PTZ- and BIC-induced tonic seizures. On the other hand, the GABA-B receptor agonist baclofen may possess a pro-convulsant effect which is caused by a presynaptic GABA-B receptor-mediated inhibition of GABA release leading to disinhibition (Motalli et al., 1999; Han et al., 2013). Therefore, GABA-B receptor antagonists are thought to be promising for treating atypical absence seizures observed in Lennox-Gastaut syndrome (Han et al., 2013). In the medial habenula GABA-B receptors are known to mediate excitation through a unique signaling mechanism which comprises amplification of presynaptic Ca^{2+} entry through Cav2.3 channels and potentiation of co-release of glutamate and acetylcholine to excite interpeduncular neurons (Zhang et al., 2016). Interestingly, fenfluramine, a positive allosteric modulator of Sig1R (Martin et al., 2020), has been shown to be clinically effective in reducing seizures in patients with Lennox-Gastaut syndrome

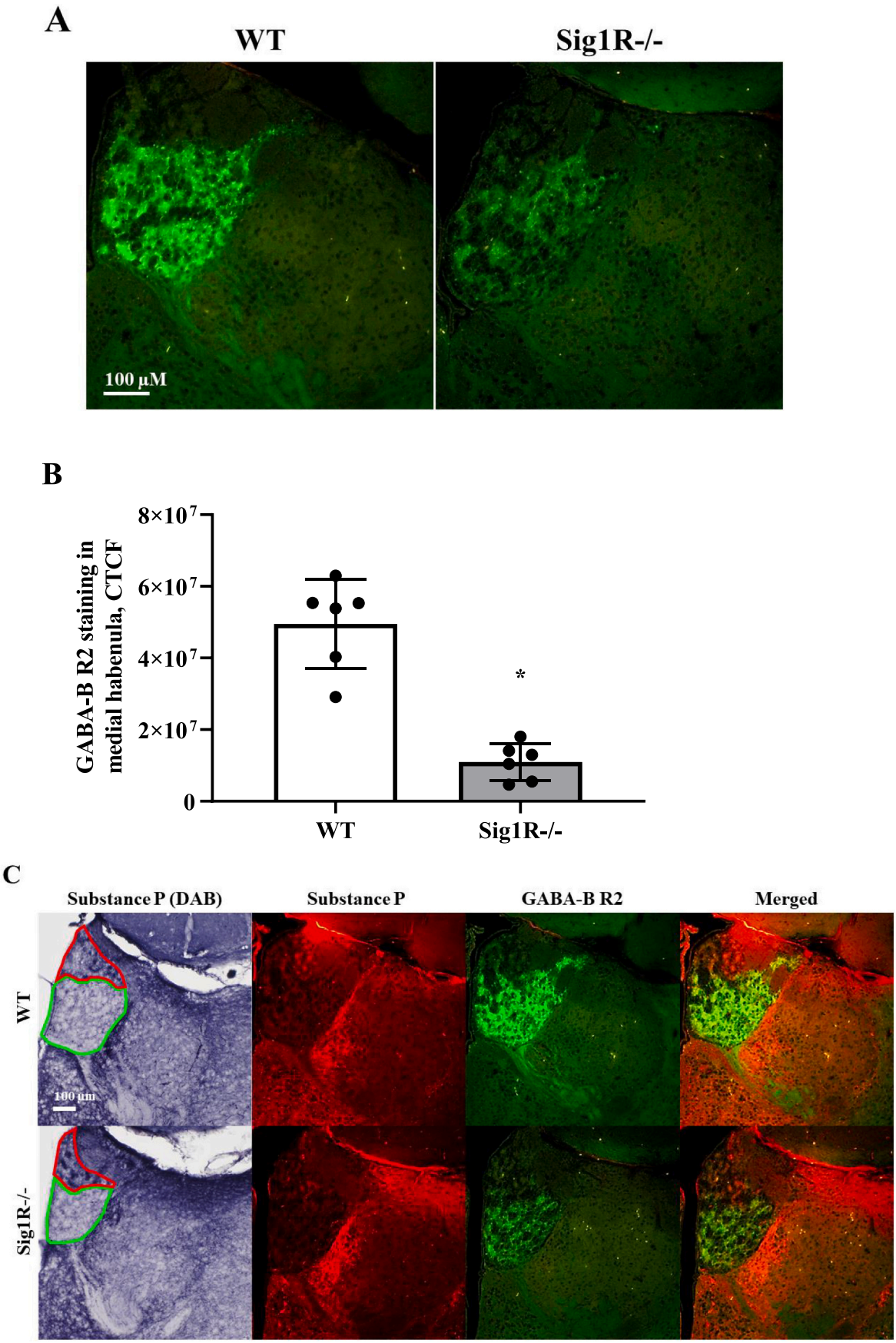

Fig. 6. Immunofluorescence of the R2 subunit of GABA-B receptors in the medial habenula. (**A**) Comparison of GABA-B R2 expression in WT and Sig1R−/− mice by using immunofluorescence, (**B**) measured corrected total cell fluorescence (CTCF). Data are expressed as the mean ± SD ($n = 6$). *$p < 0.05$ Sig1R−/− mice vs WT

mice (Mann-Whitney U test). (**C**) DAB and immunofluorescence staining of Substance P (a marker of the dorsal part of the medial habenula, red) and double immunostaining with R2 subunit of GABA-B receptors (green). Red line demonstrates dorsal part and green line demonstrates ventral part of the medial habenula. (**D**) Combined DAB and immunofluorescence staining of ChAT (a marker of the ventral part of the medial habenula) and GABA-B R2 (green), respectively. (**E**) A representative confocal image demonstrating colocalization of R1 subunit (green) and R2 subunit (red) of the GABA-B receptor in the ventral part of the medial habenula of WT and Sig1R−/− mice.

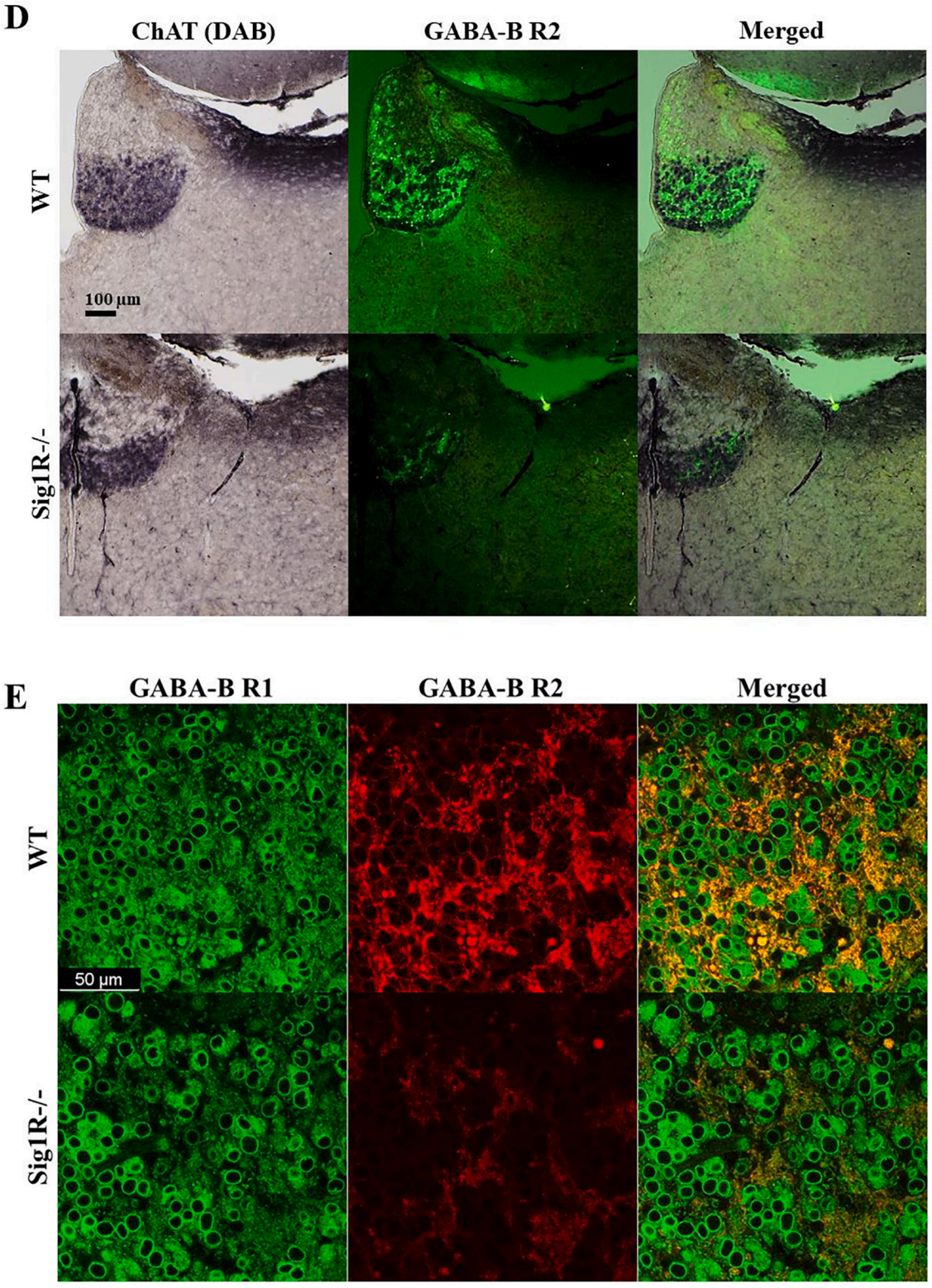

Fig. 6. (*continued*).

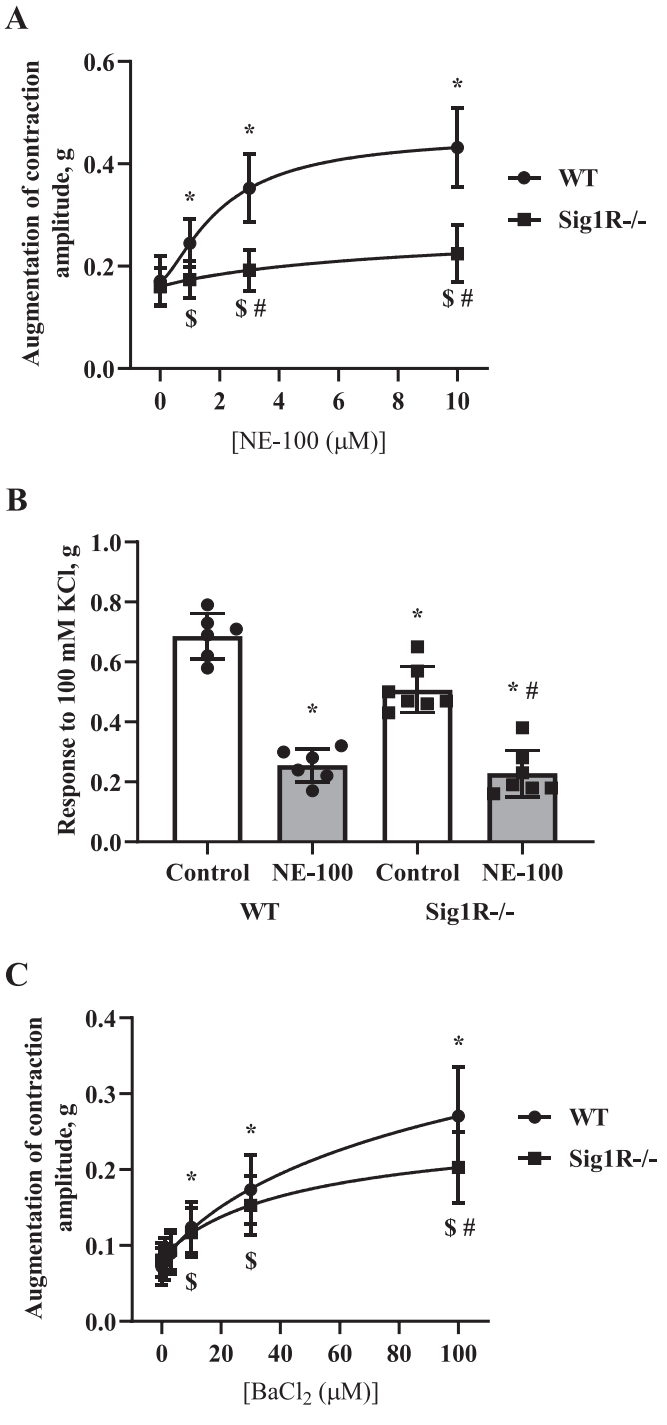

(caption on next column)

Fig. 7. Isolated *vasa deferentia* model. (**A**) NE-100-enhanced electrical current-induced contractions of *vasa deferentia*. Data are shown as the mean ± SD ($n = 6$ WT, $n = 7$ Sig1R−/− mice). $^{*}p < 0.05$ dose-dependent effect of NE-100 vs baseline of WT mice, $^{\$}p < 0.05$ dose-dependent effect of NE-100 vs baseline of Sig1R−/− mice (two-way repeated measures ANOVA followed by Dunnett's test for comparison with baseline within each group); $^{\#}p < 0.05$ WT vs Sig1R−/− (two-way repeated measures ANOVA followed by Bonferroni test for comparison of NE-100 effect between genotypes). (**B**) The effect of 10 μM NE-100 on KCl-induced maximal contractility. Data are shown as the mean ± SD (n = 6 WT, n = 7 Sig1R−/− mice). $^{*}p < 0.05$ vs WT control; $^{\#}p < 0.05$ vs Sig1R−/− control (one-way ANOVA followed by Tukey's test). (**C**) The effect of barium chloride, a nonspecific inhibitor of inward-rectifier potassium channels, on the contractility of *vasa deferentia*. Data are shown as the mean ± SD (n = 6 WT, n = 6 Sig1R−/− mice). $^{*}p < 0.05$ dose-dependent effect of barium chloride vs baseline of WT mice, $^{\$}p < 0.05$ dose-dependent effect of barium chloride vs baseline of Sig1R−/− mice (two-way repeated measures ANOVA followed by Dunnett's test for comparison with baseline within each group); $^{\#}p < 0.05$ WT vs Sig1R−/− (two-way repeated measures ANOVA followed by Bonferroni test for comparison of barium chloride effect between genotypes).

(Lagae et al., 2018), in which the most common seizure type is tonic seizures (Intusoma et al., 2013). Our data showed that Sig1R−/− mice demonstrate a significantly reduced threshold for tonic seizures, which suggests the possible role played by the Sig1R-GABA-B interaction in seizures in which the tonic component is the most common. Since GABA-B receptor-mediated mechanisms can be pro- and anti-convulsive (Joshi et al., 2016), this finding could explain the phenomena described for several Sig1R agonists and antagonists, which could also be pro- and anti-convulsive.

In the NE-100-induced seizure model, significantly reduced seizure severity was observed in Sig1R−/− animals and was presented as a lower seizure score, shorter duration and increased latency time of seizures compared to WT mice. These observations strengthen the pivotal role played by Sig1R in the control of seizures. However, the Sig1R antagonist NE-100 induced seizures not only in WT but also in Sig1R−/− animals. The mechanism of how NE-100 induces seizures is not known. We found that NE-100-induced seizures resulted in Sig1R-independent downregulation of iNOS and GABA-Aγ2 receptor subunit genes in both WT and Sig1R−/− animals, despite the different seizure severity observed in these animals after administration of NE-100. Recently, it was demonstrated that NE-100 can dose-dependently inhibit the exocytotic release of GABA and glutamate in synaptosomes isolated from rat brain (Pozdnyakova et al., 2020). In addition, bidirectional activity of NE-100 was observed on GABA uptake in rat brain synaptosomes (Pozdnyakova et al., 2020). Therefore, it seems that NE-100 dose-dependently disturbs the balance of excitation and inhibition. Since Sig1R−/− mice show decreased expression of the GABA-B R2 subunit and significantly lower seizure severity in the NE-100-induced seizure model, it is possible that the NE-100-induced seizure severity could be modulated through the level of the GABA-B R2 subunit and the activity of GABA-B receptor.

We also found that Sig1R−/− mice showed a decreased response to KCl and subsequently weaker maximal contraction in an isolated *vasa deferentia* model compared to WT animals. Recently, it was confirmed that Sig1R behaves as an atypical auxiliary subunit to modulate potassium channel function (Abraham et al., 2019). Therefore, the difference in the contractile response between WT and Sig1R−/− mice could be due to the different functions of potassium channels. It is known that activation of the postsynaptic GABA-B receptor activates inward-rectifier potassium channels (Bowery et al., 2002). The inhibitory action of Sig1R on the inward-rectifier potassium channel Kir2.1 has been previously demonstrated (Wong et al., 2016). Interestingly, the inhibition of inward-rectifier potassium channels by barium chloride results in an increase in contractions of isolated *vasa deferentia* (Diaz-Toledo and Jurkiewicz, 1991). In our study, the effect of barium chloride was less pronounced on the *vasa deferentia* isolated from Sig1R−/− mice, which confirms the role of inward-rectifier potassium channel function in this

model. Similar to barium chloride, administration of NE-100 in an isolated *vasa deferentia* model resulted in a significant dose-dependent enhancement of electrical current-induced contraction amplitude in WT mice, while there was a significantly reduced effect of NE-100 on *vasa deferentia* isolated from Sig1R−/− mice. It should be noted that Sig1R agonists PRE-084, (+)-pentazocine and antagonists BD-1047 and NE-100 were shown to similarly inhibit the KCl-induced increase in $[Ca^{2+}]_i$ in both WT and Sig1R−/− mouse brain synaptosomes and thus demonstrated Sig1R-independent effects of these ligands on KCl-induced depolarization (González et al., 2012). In keeping with previous findings, we also found a Sig1R-independent inhibitory effect of NE-100 on KCl-induced maximal contractility of WT and Sig1R−/− mouse *vasa deferentia*, which could be due to Sig1R-independent activity of NE-100 on inward-rectifier potassium channels.

5. Conclusions

Our results strongly demonstrate the reduced expression of the R2 subunit of the GABA-B receptor in the brain due to the genetic inactivation of Sig1R and supports the significance of Sig1R and GABA-B receptor cooperation in the modulation of the seizure threshold. Sig1R is a significant molecular target for seizure modulation and warrants further investigation for the development of novel anti-seizure drugs.

Declaration of Competing Interest

The international pharmaceutical company ESTEVE (headquartered in Barcelona, Spain) provided CD-1 background sigma-1 receptor knockout mice. Goat anti-mouse Abberior STAR GREEN and goat anti-rabbit Abberior STAR RED antibodies were a kind gift from Abberior Instruments (Göttingen, Germany). The authors declare that the research was conducted in the absence of any commercial or financial relationships that could be construed as potential conflicts of interest.

Acknowledgments

This study was supported by European Regional Development Fund Project No. 1.1.1.2/VIAA/2/18/376 (PostDoc Latvia), “Sigma chaperone protein as a novel drug target”. We thank Laboratorios Dr. Esteve, S.A. (Barcelona, Spain) for providing CD-1 background sigma-1 receptor knockout mice. We thank Associate Professors Inga Kadisha and Thomas van Groen (University of Alabama at Birmingham, Birmingham, Alabama, USA) for fruitful discussions regarding immunohistochemistry. We also thank Dr. biol. Dace Pjanova (Latvian Biomedical Research and Study Centre, Riga, Latvia) for the help with confocal imaging and Abberior Instruments (Göttingen, Germany) for a kind gift of fluorescently labeled Abberior STAR antibodies.

Appendix A. Supplementary data

Supplementary data to this article can be found online at https://doi.org/10.1016/j.nbd.2020.105244.

References

Abraham MJ, Fleming KL, Raymond S, Wong AYC, Bergeron R (2019). The sigma-1 receptor behaves as an atypical auxiliary subunit to modulate the functional characteristics of Kv1.2 channels expressed in HEK293 cells. Physiol rep 7. Doi: 10.14814/phy2.14147.

Alyu, F., Dikmen, M., 2017. Inflammatory aspects of epileptogenesis: contribution of molecular inflammatory mechanisms. Acta Neuropsychiatr 29, 1–16. https://doi.org/10.1017/neu.2016.47.

Bowery, N.G., Bettler, B., Froestl, W., Gallagher, J.P., Marshall, F., Raiteri, M., Bonner, T. I., Enna, S.J., 2002. International Union of Pharmacology. XXXIII. Mammalian γ-aminobutyric acidb receptors: structure and function. Pharmacol. Rev. 54, 247–264. https://doi.org/10.1124/pr.54.2.247.

Chen, L., Chan, Y.-S., Yung, W.-H., 2004. GABA-B receptor activation in the rat globus pallidus potently suppresses pentylenetetrazol-induced tonic seizures. J. Biomed. Sci. 11, 457–464. https://doi.org/10.1007/BF02256094.

Chevallier, N., Keller, E., Maurice, T., 2011. Behavioural phenotyping of knockout mice for the sigma-1 (σ1) chaperone protein revealed gender-related anxiety, depressive-like and memory alterations. J. Psychopharmacol. 25, 960–975. https://doi.org/10.1177/0269881111400648.

Couly, S., Goguadze, N., Yasui, Y., Kimura, Y., Wang, S.M., Sharikadze, N., Wu, H.E., Su, T.P., 2020. Knocking out Sigma-1 receptors reveals diverse health problems. Cell Mol Neurobiol. Online ahead of print. doi. https://doi.org/10.1007/s10571-020-00983-3.

De Sarro, G., Palma, E., Costa, N., Marra, Rosario, Gratteri, S., De Sarro, A., Rotiroti, D., 2000. Effects of compounds acting on GABA(B) receptors in the pentylenetetrazole kindling model of epilepsy in mice. Neuropharmacology 39, 2147–2161. https://doi.org/10.1016/s0028-3908(00)00050-2.

Diaz-Toledo, A., Jurkiewicz, A., 1991. Different mechanisms of action of agents acting on β-adrenoceptors in barium-stimulated and electrically-stimulated rat vas deferens. Br. J. Pharmacol. 104, 277–283. https://doi.org/10.1111/j.1476-5381.1991.tb12419.x.

Dong, L.Y., Cheng, Z.X., Fu, Y.M., Wang, Z.M., Zhu, Y.H., Sun, J.L., Dong, Y., Zheng, P., 2007. Neurosteroid dehydroepiandrosterone sulfate enhances spontaneous glutamate release in rat prelimbic cortex through activation of dopamine D1 and sigma-1 receptor. Neuropharmacology 52, 966–974. https://doi.org/10.1016/j.neuropharm.2006.10.015.

Felice, D., O’Leary, O.F., Cryan, J.F., 2016. Targeting the GABAB receptor for the treatment of depression and anxiety disorders. In: In: Receptors, Pp 219–250. Humana Press Inc.

Frangaj, A., Fan, Q.R., 2018. Structural biology of GABAB receptor. Neuropharmacology 136, 68–79. https://doi.org/10.1016/j.neuropharm.2017.10.011.

Furtinger, S., Pirker, S., Czech, T., Baumgartner, C., Sperk, G., 2003. Increased expression of γ-aminobutyric acid type B receptors in the hippocampus of patients with temporal lobe epilepsy. Neurosci. Lett. 352, 141–145. https://doi.org/10.1016/j.neulet.2003.08.046.

Galanopoulou, A.S., Moshé, S.L., 2014. Epilepsy; Experimental Models. In: In: Encyclopedia of the Neurological Sciences, Pp 112–117. Elsevier Inc.

González, L.G., Sánchez-Fernández, C., Cobos, E.J., Baeyens, J.M., Del Pozo, E., 2012. Sigma-1 receptors do not regulate calcium influx through voltage-dependent calcium channels in mouse brain synaptosomes. Eur. J. Pharmacol. 677, 102–106. https://doi.org/10.1016/j.ejphar.2011.12.029.

Gould, E.M., Curto, K.A., Craig, C.R., Fleming, W.W., Taylor, D.A., 1995. The role of GABAA receptors in the subsensitivity of Purkinje neurons to GABA in genetic epilepsy prone rats. Brain Res. 698, 62–68. https://doi.org/10.1016/0006-8993(95)00813-6.

Guo, L., Chen, Y., Zhao, R., Wang, G., Friedman, E., Zhang, A., Zhen, X., 2015. Allosteric modulation of sigma-1 receptors elicits anti-seizure activities. Br. J. Pharmacol. 172, 4052–4065. https://doi.org/10.1111/bph.13195.

Han, H.A., Cortez, M.A., Snead, O.C., 2013. GABAB receptor and absence epilepsy. In: In: Jasper’s Basic Mechanisms of the Epilepsies, Pp 242–256. Oxford University Press.

Intusoma, U., Abbott, D.F., Masterton, R.A.J., Stagnitti, M.R., Newton, M.R., Jackson, G. D., Freeman, J.L., Simon Harvey, A., Archer, J.S., 2013. Tonic seizures of Lennox-Gastaut syndrome: Periictal single-photon emission computed tomography suggests a corticopontine network. Epilepsia 54, 2151–2157. https://doi.org/10.1111/epi.12398.

Joshi, K., Cortez, M.A., Snead, O.C., 2016. Targeting the GABA B receptor for the treatment of epilepsy. In: In: Receptors, Pp 175–195. Humana Press Inc.

Kadish, I., Kumar, A., Beitnere, U., Jennings, E., McGilberry, W., van Groen, T., 2016. Dietary composition affects the development of cognitive deficits in WT and Tg AD model mice. Exp. Gerontol. 86, 39–49. https://doi.org/10.1016/j.exger.2016.05.003.

Kennedy, C., Henderson, G., 1989. An examination of the putative σ-receptor in the mouse isolated vas deferens. Br. J. Pharmacol. 98, 429–436. https://doi.org/10.1111/j.1476-5381.1989.tb12614.x.

Kilkenny, C., Browne, W., Cuthill, I.C., Emerson, M., Altman, D.G., NC3Rs Reporting Guidelines Working Group, 2010. Animal research: reporting in vivo experiments: the ARRIVE guidelines. Br. J. Pharmacol. 160, 1577–1579. https://doi.org/10.1111/j.1476-5381.2010.00872.x.

Kourrich, S., 2017. Sigma-1 receptor and neuronal excitability. In: In: Handbook of Experimental Pharmacology, Pp 109–130. Springer New York LLC.

Lagae, L., Schoonjans, A.-S., Gammaitoni, A.R., Galer, B.S., Ceulemans, B., 2018. A pilot, open-label study of the effectiveness and tolerability of low-dose ZX008 (fenfluramine HCl) in Lennox-Gastaut syndrome. Epilepsia 59, 1881–1888. https://doi.org/10.1111/epi.14540.

Langa, F., Codony, X., Tovar, V., Lavado, A., Giménez, E., Cozar, P., Cantero, M., Dordal, A., Hernández, E., Pérez, R., Monroy, X., Zamanillo, D., Guitart, X., Montoliu, L., 2003. Generation and phenotypic analysis of sigma receptor type I (σ1) knockout mice. Eur. J. Neurosci. 18, 2188–2196. https://doi.org/10.1046/j.1460-9568.2003.02950.x.

Lee, H.W., Yang, S.H., Kim, J.Y., Kim, H., 2019. The role of the medial Habenula cholinergic system in addiction and emotion-associated behaviors. Front Psychiatry 10, 100. https://doi.org/10.3389/fpsyt.2019.00100.

Liang, X., Wang, R.Y., 1998. Biphasic modulatory action of the selective sigma receptor ligand SR 31742A on N-methyl-D-aspartate-induced neuronal responses in the frontal cortex. Brain Res. 807, 208–213. https://doi.org/10.1016/s0006-8993(98)00797-5.

Lowry, O.H., Rosebrough, N.J., Farr, A.L., Randall, R.J., 1951. Protein measurement with the Folin phenol reagent. J. Biol. Chem. 193, 265–275.

Lu, C.W., Lin, T.Y., Wang, C.C., Wang, S.J., 2012. σ-1 receptor agonist SKF10047 inhibits glutamate release in rat cerebral cortex nerve endings. J. Pharmacol. Exp. Ther. 341, 532–542. https://doi.org/10.1124/jpet.111.191189.

Lüttjohann, A., Fabene, P.F., van Luijtelaar, G., 2009. A revised Racine's scale for PTZ-induced seizures in rats. Physiol. Behav. 98, 579–586. https://doi.org/10.1016/j.physbeh.2009.09.005.

Mandhane, S.N., Aavula, K., Rajamannar, T., 2007. Timed pentylenetetrazol infusion test: a comparative analysis with s.c.PTZ and MES models of anticonvulsant screening in mice. Seizure 16, 636–644. https://doi.org/10.1016/j.seizure.2007.05.005.

Martin, P., de Witte, P.A.M., Maurice, T., Gammaitoni, A., Farfel, G., Galer, B., 2020. Fenfluramine acts as a positive modulator of sigma-1 receptors. Epilepsy Behav. 105 https://doi.org/10.1016/j.yebeh.2020.106989.

Maurice, T., Su, T.-P., 2009. The pharmacology of sigma-1 receptors. Pharmacol. Ther. 124, 195–206. https://doi.org/10.1016/j.pharmthera.2009.07.001.

Maurice, T., Urani, A., Phan, V.L., Romieu, P., 2001. The interaction between neuroactive steroids and the sigma1 receptor function: behavioral consequences and therapeutic opportunities. Brain Res. Brain Res. Rev. 37, 116–132. https://doi.org/10.1016/s0165-0173(01)00112-6.

Mavlyutov, T.A., Epstein, M., Guo, L.-W., 2015. Subcellular localization of the Sigma-1 receptor in retinal neurons — an Electron microscopy study. Sci. Rep. 5, 10689. https://doi.org/10.1038/srep10689.

McGrath, J.C., Drummond, G.B., McLachlan, E.M., Kilkenny, C., Wainwright, C.L., 2010. Guidelines for reporting experiments involving animals: the ARRIVE guidelines. Br. J. Pharmacol. 160, 1573–1576. https://doi.org/10.1111/j.1476-5381.2010.00873.x.

Meldrum, B.S., 1975. Epilepsy and gamma-aminobutyric acid-mediated inhibition. Int. Rev. Neurobiol. 17, 1–36. https://doi.org/10.1016/s0074-7742(08)60205-6.

Meyer, D.A., Carta, M., Partridge, L.D., Covey, D.F., Valenzuela, C.F., 2002. Neurosteroids enhance spontaneous glutamate release in hippocampal neurons. Possible role of metabotropic sigma1-like receptors. J. Biol. Chem. 277, 28725–28732. https://doi.org/10.1074/jbc.M202592200.

Mombereau, C., Kaupmann, K., Gassmann, M., Bettler, B., van der Putten, H., Cryan, J.F., 2005. Altered anxiety and depression-related behaviour in mice lacking GABAB(2) receptor subunits. Neuroreport 16, 307–310. https://doi.org/10.1097/00001756-200502280-00021.

Motalli, R., Louvel, J., Tancredi, V., Kurcewicz, I., Wan-Chow-Wah, D., Pumain, R., Avoli, M., 1999. GABA(B) receptor activation promotes seizure activity in the juvenile rat hippocampus. J. Neurophysiol. 82, 638–647. https://doi.org/10.1152/jn.1999.82.2.638.

Perucca, P., Scheffer, I.E., Kiley, M., 2018. The management of epilepsy in children and adults. Med. J. Aust. 208, 226–233.

Pozdnyakova, N., Krisanova, N., Dudarenko, M., Vavers, E., Zvejniece, L., Dambrova, M., Borisova, T., 2020. Inhibition of sigma-1 receptors substantially modulates GABA and glutamate transport in presynaptic nerve terminals. Exp. Neurol. 333, 113434. https://doi.org/10.1016/j.expneurol.2020.113434.

Reddy, D.S., Kulkarni, S.K., 1998. Proconvulsant effects of neurosteroids pregnenolone sulfate and dehydroepiandrosterone sulfate in mice. Eur. J. Pharmacol. 345, 55–59. https://doi.org/10.1016/s0014-2999(98)00034-x.

Sabino, V., Cottone, P., Parylak, S.L., Steardo, L., Zorrilla, E.P., 2009. Sigma-1 receptor knockout mice display a depressive-like phenotype. Behav. Brain Res. 198, 472–476. https://doi.org/10.1016/j.bbr.2008.11.036.

Sha, S., Qu, W.J., Li, L., Lu, Z.H., Chen, L., Yu, W.F., Chen, L., 2013. Sigma-1 receptor knockout impairs neurogenesis in dentate gyrus of adult hippocampus via down-regulation of nmda receptors. CNS Neurosci Ther 19, 705–713. https://doi.org/10.1111/cns.12129.

Su, T.-P., Su, T.-C., Nakamura, Y., Tsai, S.-Y., 2016. The Sigma-1 receptor as a pluripotent modulator in living systems. Trends Pharmacol. Sci. 37, 262–278. https://doi.org/10.1016/j.tips.2016.01.003.

Terunuma, M., 2018. Diversity of structure and function of GABAB receptors: a complexity of GABAB-mediated signaling. Proc Japan Acad Ser B Phys Biol Sci 94, 390–411. https://doi.org/10.2183/pjab.94.026.

Vavers, E., Svalbe, B., Lauberte, L., Stonans, I., Misane, I., Dambrova, M., Zvejniece, L., 2017. The activity of selective sigma-1 receptor ligands in seizure models in vivo. Behav. Brain Res. 328, 13–18. https://doi.org/10.1016/j.bbr.2017.04.008.

Vavers, E., Zvejniece, L., Maurice, T., Dambrova, M., 2019. Allosteric modulators of sigma-1 receptor: a review. Front. Pharmacol. 10, 223. https://doi.org/10.3389/fphar.2019.00223.

Viswanath, H., Carter, A.Q., Baldwin, P.R., Molfese, D.L., Salas, R., 2014. The medial habenula: still neglected. Front. Hum. Neurosci. 7 https://doi.org/10.3389/fnhum.2013.00931.

Wong, A.Y.C., Hristova, E., Ahlskog, N., Tasse, L.A., Ngsee, J.K., Chudalayandi, P., Bergeron, R., 2016. Aberrant subcellular dynamics of sigma-1 receptor mutants underlying neuromuscular diseases. Mol. Pharmacol. 90, 238–253. https://doi.org/10.1124/mol.116.104018.

Zhang, J., Tan, L., Ren, Y., Liang, J., Lin, R., Feng, Q., Zhou, J., Hu, F., Ren, J., Wei, C., Yu, T., Zhuang, Y., Bettler, B., Wang, F., Luo, M., 2016. Presynaptic excitation via GABAB receptors in Habenula cholinergic neurons regulates fear memory expression. Cell 166, 716–728. https://doi.org/10.1016/j.cell.2016.06.026.

Zhang, B., Wang, L., Chen, T., Hong, J., Sha, S., Wang, J., Xiao, H., Chen, L., 2017. Sigma-1 receptor deficiency reduces GABAergic inhibition in the basolateral amygdala leading to LTD impairment and depressive-like behaviors. Neuropharmacology 116, 387–398. https://doi.org/10.1016/j.neuropharm.2017.01.014.

Zvejniece, L., Svalbe, B., Makrecka, M., Liepinsh, E., Kalvinsh, I., Dambrova, M., 2010. Mildronate exerts acute anticonvulsant and antihypnotic effects. Behav. Pharmacol. 21, 548–555. https://doi.org/10.1097/FBP.0b013e32833d5a59.